

This is the peer reviewed version of the following article:

Bader, C. and Sorvina, A. and Simpson, P. and Wright, P. and Stagni, S. and Plush, S. and Massi, M. et al. 2016. Imaging nuclear, endoplasmic reticulum, and plasma membrane events in real time. FEBS Letters.,

which has been published in final form at <http://doi.org/10.1002/1873-3468.12365>

This article may be used for non-commercial purposes in accordance with Wiley Terms and Conditions for Self-Archiving at <http://olabout.wiley.com/WileyCDA/Section/id-820227.html#terms>

1 **Imaging nuclear, endoplasmic reticulum and plasma membrane events in** 2 **real time**

3 Christie A. Bader¹, Alexandra Sorvina¹, Peter V. Simpson², Phillip J. Wright², Stefano
4 Stagni³, Sally E. Plush¹, Massimiliano Massi², Douglas A. Brooks^{1*}

5 ¹Mechanisms in Cell Biology and Disease Research Group, School of Pharmacy and Medical
6 Sciences, Sansom Institute for Health Research, University of South Australia, Adelaide,
7 Australia.

8 ²Department of Chemistry and Nanochemistry Research Institute, Curtin University, Bentley,
9 Australia.

10 ³Department of Industrial Chemistry “Toso Montanari”, University of Bologna, Bologna,
11 Italy.

12

13 **Abstract**

14 Live cell imaging can provide important information on cellular dynamics, however the full
15 utilisation of this technology has been hampered by the limitation imaging reagents. Metal-
16 based complexes have the potential to overcome many of the issues common to many current
17 imaging agents. The rhenium (I) based complex *fac*-[Re(CO)₃(1,10-phenanthroline)(4-
18 pyridyltetrazolate)], herein referred to as ReZolve-ERTM, shows promise as a live cell
19 imaging agent with rapid cell uptake, low cytotoxicity, resistance to photobleaching and
20 compatibility with multicolour imaging. ReZolve-ERTM localised to the nuclear
21 membrane/endoplasmic reticulum (ER) and allowed the detection of exocytotic events at the
22 plasma membrane. Thus, we present a new imaging agent for monitoring live cell events in
23 real time, which is ideal for imaging either short or long time courses.

24

25 **Introduction**

26 One of the most exciting advances in cell biology has been the development of technology
27 for live cell imaging, which enables the visualisation of molecular events in real time.
28 However, while there have been significant advances in spatial and temporal resolution
29 imaging, with for example spinning disk, fast scanning and super resolution microscope
30 technologies [1,2], the field of imaging reagents has struggled to keep pace. This is partially
31 because the imaging reagent market is undergoing a quantum shift from imaging reagents
32 that require cell fixation, which is known to generate significant artefacts [3], to those that
33 enable real time live cell imaging. Reagents for live cell imaging ideally should exhibit *in situ*
34 stability, optimal emission/photophysical properties, a large Stokes shift, resistance to
35 photobleaching, capacity for multicolour/multiple probe imaging and most importantly low
36 toxicity [4]. Consequently, there is a very high demand for imaging reagents that meet these
37 criteria to enable effective live cell imaging without perturbing cellular mechanisms.

38

39 There are a range of technical approaches for live cell imaging, including endogenous
40 fluorescence, genetic expression systems, quantum dots and small fluorescent molecules.

41 Endogenous fluorescence has been effectively used for *in vitro* live cell and *intravital*
42 imaging [5,6], and while this mode of imaging does not require exogenous labelling there are
43 only a limited number of molecules capable of generating detectable endogenous
44 fluorescence [7]. Furthermore, endogenous fluorescence (often referred to as
45 autofluorescence) can actually be a hindrance when combined with specific microscopy
46 imaging techniques [8]. While GFP expression systems revolutionised the field of
47 mammalian cell biology [9,10], this technology requires genetic manipulation of the target.
48 Moreover, the GFP molecule is large and can cause steric problems that influence molecular
49 function [11]. In addition, many molecular targets, including carbohydrates and lipids are not
50 amenable to this technology. While the use of quantum dot imaging is rapidly increasing, this
51 nanocrystal technology can be prone to particle breakdown, toxicity and high production
52 costs [12]. To date the majority of the commercially available reagents for fluorescence
53 imaging have been based on organic compounds, like BODIPY. These compounds can suffer
54 from a range of issues including concentration dependent fluorescent shifts, photobleaching
55 and cytotoxicity. To address the growing need for specific, high quality imaging reagents that
56 do not affect cell viability, researchers have been exploring luminescent metal complexes,
57 such as those of Re(I), Ru(II), Ir(III), Pt(II) and the trivalent lanthanides [13-16]. Metal
58 complexes have the potential to overcome a number of the pitfalls associated with organic
59 fluorophores, as they are typically resistant to photobleaching, allowing excitation for longer
60 periods of times with respect to organic fluorophores. Moreover, the triplet multiplicity
61 nature of the excited states of these species implies that their excited state lifetime is usually
62 elongated, ranging between hundreds of nanoseconds to milliseconds depending on the
63 structure of the complex. Compared to the fast decay of endogenous autofluorescence, the
64 transition metal characteristics can be exploited in time-gated imaging techniques, to
65 improve signal-to-noise ratios. Lastly, the large Stokes shift of luminescent metal
66 complexes is beneficial to avoid issues with concentration dependent quenching.

67

68 Recently, we have shown that the Re(I) complex *fac*-[Re(CO)₃(**phen**)(L^{3py})], where **phen** is
69 1,10-phenanthroline and L^{3py} is 3-pyridyltetrazolate can be utilised for live cell imaging, and
70 it localises to acidic vesicles [17]. This complex was also found to be highly resistant to
71 photobleaching, strongly emissive with a large Stokes shifts and long emission life times,
72 whilst exhibiting minimal to no cytotoxicity [17]. We have also shown that changes to the
73 tetrazolate structure result in changes in intracellular distribution, whilst retaining the key
74 properties for live cell imaging (photobleaching resistant, large Stokes shift, minimal
75 cytotoxicity). For example the exchange of the L^{3py} for 4-cyanophenyltetrazolate results in
76 Re(I) complex (ReZolve-L1TM) with shown preferential localisation within the lipid droplet
77 [17,18]. Therefore, in the interest of designing new Re(I) complexes for cell imaging, we
78 furthered our investigation of altering the chemical nature of the ancillary ligand to highlight
79 consequent effects in biological behaviour of the metal-based complex. We have previously
80 published the synthesis, electrochemical and photophysical properties of the analogous Re(I)
81 complex bound to the 4-pyridyltetrazolate ligand, herein designated as ReZolve-ERTM [19].
82 Remarkably, preliminary investigation into the incubation and localisation of this complex
83 revealed a different staining pattern with respect to *fac*-[Re(CO)₃(**phen**)(L^{3py})], despite the
84 only difference between the two complexes being the 3- or 4-pyridyl substituent. Intrigued by
85 this initial finding we continued our investigation and here we show that ReZolve-ERTM

86 localises to the endoplasmic reticulum (ER) [17]. Furthermore we show that ReZolve-ERTM
87 is ideal for live cell imaging applications, with rapid detection within cells, resistance to
88 photobleaching, consistent cellular localisation and low cytotoxicity. In addition, ReZolve-
89 ERTM allowed the visualisation of specific nuclear events, ER structures and vesicle release
90 from the cell surface, demonstrating that this compound is suitable for investigating a range
91 of biological questions related to cellular dynamics.

92

93 **Materials and Methods**

94 **Cell culture and staining**

95 The non-malignant cell lines PNT1a and PNT2 and prostate cancer cell line LNCaP (clone
96 FCG) were obtained from the European Collection of Cell Cultures via CellBank Australia
97 (Children's Medical Research Institute, NSW, Australia). Prostate cancer cell line DU145,
98 was obtained from the American Tissue Culture Collection via Cryosite (Cryosite Ltd., New
99 South Wales, Australia). Chinese hamster ovaries CHO-K1 cell line and Human monocytic
100 leukemia THP-1 cell line were obtained from the American Type Culture Collection via
101 Sigma-Aldrich (Sigma-Aldrich, St. Louis, USA).

102

103 The PNT1a, PNT2, CHO-K1 and THP-1 cell lines were maintained in Roswell Park
104 Memorial Institute (RPMI) 1640 culture medium (Sigma-Aldrich, USA), supplemented with
105 10% foetal calf serum (In Vitro Technologies, Australia), 2 mM L-glutamine (Sigma-Aldrich,
106 USA). The DU-145 cell line was cultured in minimum essential medium (Gibco, Life
107 Technologies, USA), supplemented with 10% foetal calf serum, 2 mM L-glutamine and 1
108 mM sodium pyruvate (Sigma-Aldrich, USA). The LNCaP cell line was cultured in RPMI-
109 1640 media (Gibco, Life Technologies, USA) supplemented with 2 mM L-glutamine, 10 %
110 FCS, 10 mM HEPES (Sigma-Aldrich, USA) and 1 mM sodium pyruvate. THP-1 monocytes
111 were differentiated into macrophages by incubation with RPMI-1640 medium containing 5
112 ng/mL of phorbol 12-myristate 13-acetate (Sigma-Aldrich, USA) over 48 hours. Cells were
113 cultured to approximately 90% confluence before passage, by washing with sterile PBS
114 (Sigma-Aldrich, St. Louis, USA), TrypLETM Express (Gibco, USA) to dissociate the cells
115 from the culture surface and then resuspended in supplemented culture medium. Cell lines
116 were maintained at 37°C and 5% CO₂ in a Sanyo MCO-17AI humidified incubator (Sanyo
117 Electric Biomedical, Japan). For imaging experiment cells were culture in Ibidi μ -slides 8
118 wells (Ibidi, Germany) and for MTS assays PNT2 cells were cultured in 96 well plates.

119

120 For cellular imaging, cells were incubated with 50 μ M ReZolve-ERTM prepared in serum free
121 cell culture media, from a 10 mM stock solution prepared in DMSO. Cells were then imaged
122 immediately or following 15 min of incubation without washing cells. For co-staining
123 experiments cell were stained with ER-Tracker[®] Red, MitoTracker[®] Red CMXRos,
124 LysoTracker[®] Red DND-99 or CellMaskTM (Molecular Probes, USA), according to the
125 manufactures instructions. Cells were then washed 2 x 30 sec in PBS. Serum free media
126 containing 50 μ M of ReZolve-ERTM was then added and images were collected after 15
127 minutes of incubation. Cell fixation was performed using 4% paraformaldehyde in PBS for

128 20 minutes at room temperature. Cells were then washed for 3 x 10 minutes in PBS before
129 incubation with 50 μ M ReZolve-ERTM for 20 minutes.

130

131 **Confocal imaging and analysis**

132 For confocal imaging cells were held in a Uno-Combined-Controller, CO₂ microscope
133 electric top stage incubation system (Okolab, Italy) held at 37°C and 5% CO₂. Confocal
134 imaging was performed on a Nikon A1⁺ confocal microscope, fitted with a LU-N4/LU-N4S
135 4-laser unit (405 nm, 488 nm, 561 nm, 640 nm), the A1-DUG GaAsP Multi Detector Unit (2
136 GaAsP PMTs + 2 standard PMTs) and a 32 channel spectral detector (Nikon, Japan). Images
137 were captured using a 60x oil emersion lens. Each confocal micrograph represented 0.5 μ m
138 thin optical sections.

139

140 To assess emission intensity of ReZolve-ERTM over time NIS-Elements software (Nikon,
141 Japan) was used. Regions of interest were selected using the AutoDetect function to select
142 cells containing ReZolve-ERTM, mean emission intensity was then measured over time for
143 each region of interest. For each experiment greater than six regions of interest were used to
144 gain the average emission intensity in Microsoft Excel 2013 (which were then plotted against
145 time). Co-localisation between ReZolve-ERTM and ER-Tracker® Red, MitoTracker® Red
146 CMXRos or LysoTracker® Red DND-99 was assessed in NIS-Elements software (Nikon,
147 Japan) using the co-localisation analysis to generate a Pearson's correlation coefficient. Cells
148 from a minimum of 10 images for each marker were measured for co-localisation and the
149 means were compared by ANOVA analysis in GraphPad Prism with Tukey post-hoc analysis
150 (Prism software, version 6.01, USA).

151 **Cytotoxicity assay**

152 To assess cytotoxicity of the complexes, cellular NAD(P)H-dependent redox activity was
153 measured using CellTiter 96[®] Aqueous Non-Radioactive Cell Proliferation Assay (MTS)
154 according to the manufacturer instruction (Promega, USA). Briefly, PNT2 cells were cultured
155 as described above in 96 well plates for 24 h. Cells were then incubated with 50 μ M of
156 ReZolve-ERTM for 1 h, 4 h, 8 h or 24 h in serum free media, for a control cells were incubate
157 with 0.5% v/v DMSO in serum free media for the corresponding incubation time without the
158 presence of ReZolve-ERTM. Media was then removed and replaced by 120 μ L of MTS and
159 PMS in RPMI-1640 medium and allowed to incubate at room temperature for 1 h. The
160 absorbance was then measured at 490 nm by EnSpire Plate Readers (PerkinElmer, USA).

161

162 **Results and discussion**

163 The synthesis and photophysical properties of ReZolve-ERTM have previously been reported
164 [19]. This complex was found to be compatible with fluorescent microscopy using single
165 photon excitation at 403 nm or two-photon excitation between 800 nm and 830 nm, making it
166 amenable for use with a range of microscopy set ups and applications.

167

168 ***ReZolve-ERTM cellular uptake is by passive diffusion.***

169 For effective cellular imaging, reagents need to penetrate the cell membrane and accumulate
170 in a cell at a high enough concentration for detection by fluorescence microscopy. To assess
171 this, live non-malignant prostate PNT2 cells were incubated with ReZolve-ERTM at 50 μ M,
172 and the emission monitored in real time over 30 minutes (Supplementary Video 1). Using a
173 Nikon A1 microscope (equipped with a live cell incubator), the emission from ReZolve-
174 ERTM was detected within seconds after the complex was applied, using a low excitation
175 power (403 nm excitation laser set to < 2 power setting) and a low detector sensitivity (Si
176 PMT HV detector 180). Initially ReZolve-ERTM could be detected in the cytoplasm, but
177 within the first minute of addition, the accumulation of the complex could be detected in the
178 peri-nuclear region. The emission intensity increased throughout the cell over the first 10
179 minutes. After this time, the intensity and localisation of the complex appeared to be
180 consistent for the next 20 minutes of image collection. The ability to detect the complex in
181 cells within seconds of addition, at low laser power, is important as this will prevent photo-
182 damage of live cells and suggested the potential for ReZolve-ERTM as a real time imaging
183 agent.

184

185 The rapid entry of ReZolve-ERTM into PNT2 cells suggested that this complex was able to
186 freely transit across the cell membrane. Furthermore, the signal from the ReZolve-ERTM was
187 concentration dependent, and a concentration of 50 μ M was optimal for imaging, with lower
188 concentrations resulting in weaker signal detection. When cells that had been labelled with
189 ReZolve-ERTM were washed (i.e. media containing ReZolve-ERTM was replaced with fresh
190 culture medium containing no dye), there was an immediate reduction in the ReZolve-ERTM
191 detection. This suggested that ReZolve-ERTM had a low affinity for its cellular target; and
192 supported the premise that a passive diffusion mechanism was involved for ReZolve-ERTM
193 cell entry, as this mechanism is dependent on a concentration gradient. To further confirm
194 this mode of entry, cells were fixed in paraformaldehyde and incubated with ReZolve-ERTM.
195 The complex could be easily detected in these cells following fixation, confirming passive
196 transport as the mode of cell entry (Supplementary figure 1). The rapid uptake of ReZolve-
197 ERTM is ideal for real time imaging of cells and the ability to control the addition or removal
198 of the complex may be well suited to the long term monitoring of specific cellular structures.

199

200 To assess the photostability of ReZolve-ERTM in cells, PNT2 cells were incubated with the
201 complex and imaged continuously using a higher laser power, in an attempt to induce
202 photobleaching. Images were collected with a scan rate of 0.22 seconds and a pixel dwell
203 time of 0.22 milliseconds for a total of 448 scans (approximately 29 minutes), with the
204 excitation power set to a setting of 10, which was five times greater than the maximum power
205 required for ReZolve-ERTM visualisation. Over the first eight minutes of image collection the
206 intensity increased as the complex accumulated in cells (Figure 1), as was observed when a
207 lower laser power was used (Supplementary video 1). Between eight and 29 minutes the
208 emission intensity remained constant (Figure 1); suggesting that the complex was highly
209 resistant to photobleaching. However, an increase in emission intensity was observed in the
210 final minutes of acquisition when using a high laser power (five times the power required for
211 visualisation), indicating that photo-activation may be occurring.

212

213 ***ReZolve-ERTM is detected at the ER and nucleoplasmic reticulum.***

214 In different cell lines, including non-malignant prostate cells (PNT2 and PNT1a), malignant
215 prostate cancer cells (LNCaP and DU145), CHO-K1 cells and THP-1 macrophages
216 (Supplementary Figure 2), ReZolve-ERTM detected a central structure within the nucleus that
217 resembled the nucleolus, with projections towards the nuclear membrane; as well as a diffuse
218 reticular network emanating from the nuclear region, which extended into distal regions of
219 the cell. To further define this intracellular distribution, ReZolve-ERTM was co-stained with
220 ER-Tracker® (ER), MitoTracker® (mitochondria), LysoTracker® (lysosomes/acidic vesicles)
221 and CellMaskTM (plasma membrane) in PNT2 cells. PNT2 cells were labelled with the latter
222 commercial dyes, the cells were briefly washed and then incubated with 50 µM ReZolve-
223 ERTM for 15 to 20 minutes before imaging (Figure 2). ReZolve-ERTM showed significant co-
224 localisation with ER-Tracker®, with a Pearson's correlation coefficient of 0.84 ± 0.01 . Co-
225 localisation between ReZolve-ERTM and ER-Tracker® was observed on the reticular network
226 extending from the nucleus into the cytoplasm, at the nuclear membrane and on membranous
227 structures extending into the nucleus that appear to be nucleoplasmic reticulum (Figure 2A).
228 The nucleoplasmic reticulum has been previously visualised using ER markers, such as ER-
229 Tracker® [20, 21] or ER associated Ca²⁺-ATPase [22], which was consistent with ReZolve-
230 ERTM detecting a similar, biologically related structure. In contrast, there was only a limited
231 amount of ReZolve-ERTM detected in association with mitochondria (Figure 2B) and
232 lysosomes (Figure 2C), which was shown by lower Pearson's correlation coefficients for co-
233 localisation between ReZolve-ERTM and either MitoTracker® or LysoTracker® of 0.44 ± 0.01
234 or 0.37 ± 0.01 , respectively. While most of the mitochondrial and lysosomal labelling was
235 independent of ReZolve-ERTM some overlap was detected between these structures (Figure
236 2B, 2C). This overlap between ReZolve-ERTM and mitochondria or lysosomes was not
237 surprising given the close association between the ER and these two subcellular
238 compartments [23, 24]. Interestingly, while ReZolve-ERTM did not stain large areas of the
239 plasma membrane (Figure 2; i.e. limited co-localisation with CellMaskTM), there was some
240 specific sites of co-localization with CellMaskTM (Figure 5B), which may have identified a
241 localised interaction between the endoplasmic reticulum and the cell surface.

242 From this co-location study we propose that ReZolve-ERTM locates to the ER and
243 biologically related structures, in live cells. The mechanism by which ReZolve-ERTM
244 associates with the nuclear membrane/ER is not currently known, but a similar tricarbonyl
245 rhenium(I) diimine luminescent complex, ReZolve-L1TM, has been shown to localise with
246 polar lipids in cells [17, 18]. Given that the ER is a major site of lipid synthesis [25], we can
247 speculate that ReZolve-ERTM may have a similar lipophilic interaction.

248

249 ***ReZolve-ERTM remains in ER structures during longer term real time imaging.***

250 For long term imaging experiments it is important for a reagent to be retained in cells over a
251 long period of time, and to cause minimal to no damage to the cells. PNT2 cells were
252 incubated with ReZolve-ERTM and imaged for 280 minutes at 10 minute intervals to assess
253 the compatibility of the complex with long term imaging. Over 280 minutes ReZolve-ERTM
254 remained localised to the perinuclear region of cells (Figure 3A-C). Although the intensity of

255 the emission from ReZolve-ERTM decreased over time, it was still easily detected at the end
256 of the time course (Figure 3C, 3D). The decrease in emission intensity was likely due to the
257 complex being slowly trafficked out of the cell, and not related to photobleaching, as the
258 complex was photo-resistant and exhibited continuous emission in response to extended laser
259 exposure (Figure 3). To assess the potential cytotoxic effects of ReZolve-ERTM, PNT2 cells
260 were incubated with the complex for 1, 4, 7 or 24 hours and the cell viability assessed via an
261 MTS assay (Figure 3E). Cell viability (as indicated by absorbance) was reduced when treated
262 with ReZolve-ERTM at 50 μ M for 1 hour and 4 hours compared to controls, however the
263 viability was still significantly higher than the negative control (Figure 3E). Although cell
264 viability was reduced by this complex, cells imaged with ReZolve-ERTM for the 4 hours did
265 not show morphological changes, which would have indicated cytotoxicity during this time,
266 thus suggesting that the cytotoxicity of ReZolve-ERTM was low. Interestingly, following 7
267 hours and 24 hours of incubation with ReZolve-ERTM the cell viability was unchanged when
268 compared to controls (Figure 3E). While this may be due to complex efflux, it showed that
269 long term exposure to the ReZolve-ERTM does not affect overall cell survival. The minimal
270 cytotoxic effects of ReZolve-ERTM and its ability to be detected in cells over a long time
271 periods make this complex an ideal tool for live cell imaging.

272

273 ***Detection of nuclear and ER events with ReZolve-ERTM.***

274 A number of time series images were collected using ReZolve-ERTM (Figures 4 and 5) and
275 these revealed inward projections from the nuclear membrane, which resembled a phagocytic
276 event at the nuclear membrane (Figure 4), as well as a number of small vesicles in the cellular
277 periphery (Figure 5). Figure 4 shows that ReZolve-ERTM detected the formation of a large \sim 3
278 μ m nuclear membrane derived phagosome that appeared to sequester part of the nucleoplasm
279 (Supplementary Video 2). ReZolve-ERTM clearly defined the nuclear membrane extension as
280 well as the phagosome vesicle formation, closure and release event, which was evident
281 during the 5 minute imaging time course. It is generally accepted that trafficking into and out
282 of the nucleus occurs through nuclear pores, which is facilitated by the nuclear pore complex
283 [26], but budding and formation of vesicles can also occur from the nuclear envelope [27-29].
284 For example, ribonucleoprotein particles can be exported out of the nucleus in a process
285 similar to viral capsid nuclear egress, where small vesicles have been observed forming at the
286 nuclear envelop, before budding out to release their content [27]. In TEM images
287 multivesicular bodies have also been visualised in close proximity to the nuclear envelope
288 and in some cases these multivesicular structures appeared to be forming from the nuclear
289 envelope [28,29]. Although the identity of this nuclear structure is unclear, and we cannot
290 rule out an artificially induced cellular response to the complex, it seemed that ReZolve-
291 ERTM was able to visualise specific nuclear events in real time, indicating its potential for live
292 cell imaging applications.

293

294 To further explore the detection of small ($<$ 0.5 μ m) vesicles by ReZolve-ERTM in the cellular
295 periphery, a dual labelling time-course experiment was performed using both ReZolve-ERTM
296 and CellMaskTM. This enabled the simultaneous visualisation of two distinct vesicular events
297 at the cell surface (Figure 5; Supplementary Video 3). CellMaskTM identified a \sim 1 μ m
298 diameter vesicle forming over an eight minute time course, involving a membrane protrusion

299 from the cell surface and then vesicle budding/excision from the plasma membrane; and
300 interestingly this microvesicle contained a small amount of diffuse ReZolve-ERTM staining in
301 its lumen (Figure 5B). The detection of ReZolve-ERTM inside the budding vesicle (Figure 5B)
302 could be consistent with the dissociation of the dye from the membrane into the vesicle (N.B.
303 cell washing significantly reduced the staining, suggesting that ReZolve-ERTM has a low
304 affinity for its target); however we could not exclude the possibility that ReZolve-ERTM was
305 identifying a specific target within these budding vesicles. In addition, a small (< 0.5 μm)
306 vesicle with intense ReZolve-ERTM staining was visualised: first distorting a specific location
307 on the plasma membrane and showing co-location with CellMaskTM; and then pushing
308 through the plasma membrane to be released from the cell (Figure 5C). This later event
309 occurred more rapidly (~ 2-3 minutes) when compared to the former 1 μm diameter vesicle
310 formation and release (~ 8-9 minutes). These observations suggest that ReZolve-ERTM has
311 the potential for not only visualising the ER, but also vesicle trafficking out of the cell.

312

313 **Conclusion**

314 Visualising cellular organelles such as the ER can provide powerful insights for
315 understanding cellular dynamics under a range of physiological conditions. The ER plays a
316 central role in protein transcription, molecular trafficking and cellular signalling.
317 Endoplasmic reticulum stress is commonly observed in a range of diseases and in response to
318 physiological stress, and thus the ability to track the ER over large time periods may provide
319 new insights into diseases such as cancer, non-alcoholic fatty liver disease, diabetes and
320 neurodegenerative disease. Thus an imaging reagent such as ReZolve-ERTM that can monitor
321 the ER has potential applications in facilitating our understanding of cell biology in a range
322 of diseases. Given that ReZolve-ERTM has the ability to be used over short or long time
323 courses, is highly resistant to photobleaching, can be removed from cells, has low
324 cytotoxicity over long exposure times and has already demonstrated its ability to detect
325 interesting cellular phenomena in real time, this imaging reagent could be utilised in a
326 multitude of experimental protocols and provide a flexible imaging tool for cell biologists.

327

328 **Acknowledgements.**

329 This work was supported by funding from the University of South Australia, an ITEK
330 catalyst grant and a BioSA Innovation grant awarded to DAB, SP and MM. MM also wishes
331 to thank the ARC for funding (FT130100033). The authors declare a financial interest in
332 ReZolve-ERTM as this imaging agent is being commercialized by ReZolve Scientific.

333

334 **Author contribution**

335 CB, SP, MM and DB conceived and supervised the study; CB SP and DB designed
336 experiments; CB and AS performed experiments; PS, PW and SS provided and characterised
337 new tools and reagents; CB, SP and DB wrote the manuscript; AS, PS, PW, SS and MM
338 made manuscript revisions.

339

340 References
341

- 342 1. Nakano A (2002) Spinning-disk confocal microscopy- A cutting-edge tool for imaging of membrane
343 traffic. *Cell Struct Funct* 27: 349-355.
- 344 2. Hell SW (2009) Microscopy and its focal switch. *Nat Meth* 6: 24-32.
- 345 3. Rastogi V, Puri N, Arora S, Kaur G, Yadav L, et al. (2013) Artefacts: A diagnostic dilemma. *J Clin*
346 *Diagn Res* 7: 2408-2413.
- 347 4. Ettinger A, Wittmann T (2014) Chapter 5 - Fluorescence live cell imaging. In: Jennifer CW, Torsten
348 W, editors. *Methods Cell Bio: Academic Press*. pp. 77-94.
- 349 5. Shandala T, Lim C, Sorvina A, Brooks D (2013) A *Drosophila* model to image phagosome
350 maturation. *Cells* 2: 188.
- 351 6. Zipfel WR, Williams RM, Christie R, Nikitin AY, Hyman BT, et al. (2003) Live tissue intrinsic emission
352 microscopy using multiphoton-excited native fluorescence and second harmonic generation.
353 *Proc Natl Acad Sci USA* 100: 7075-7080.
- 354 7. Croce AC, Bottiroli G (2014) Autofluorescence spectroscopy and imaging: A tool for biomedical
355 research and diagnosis. *Eur J Histochem* 58: 2461.
- 356 8. Yang Y, Honaramooz A (2012) Characterization and quenching of autofluorescence in piglet testis
357 tissue and cells. *Anat Res Inter*.
- 358 9. Chalfie M, Tu Y, Euskirchen G, Ward WW, Prasher DC (1994) Green fluorescent protein as a
359 marker for gene expression. *Science* 263: 802-805.
- 360 10. Heim R, Prasher DC, Tsien RY (1994) Wavelength mutations and posttranslational autoxidation of
361 green fluorescent protein. *Proc Natl Acad Sci USA* 91: 12501-12504.
- 362 11. Kuruppu S, Tochon-Danguy N, Ian Smith A (2013) Applicability of green fluorescence protein in
363 the study of endothelin converting enzyme-1c trafficking. *Protein Sci* 22: 306-313.
- 364 12. Zhu Z-J, Yeh Y-C, Tang R, Yan B, Tamayo J, et al. (2011) Stability of quantum dots in live cells. *Nat*
365 *Chem* 3: 963-968.
- 366 13. New EJ, Congreve A, Parker D (2010) Definition of the uptake mechanism and sub-cellular
367 localisation profile of emissive lanthanide complexes as cellular optical probes. *Chem Sci* 1:
368 111-118.
- 369 14. Baggaley E, Weinstein JA, Williams JAG (2012) Lighting the way to see inside the live cell with
370 luminescent transition metal complexes. *Coord Chem Rev* 256: 1762-1785.
- 371 15. Coogan MP, Fernandez-Moreira V (2014) Progress with, and prospects for, metal complexes in
372 cell imaging. *Chem Commun* 50: 384-399.
- 373 16. Lo KK-W (2015) Luminescent rhenium(I) and iridium(III) polypyridine complexes as biological
374 probes, imaging reagents, and photocytotoxic Agents. *Acc Chem Res* 48: 2985-2995.
- 375 17. Bader CA, Brooks RD, Ng YS, Sorvina A, Werrett MV, et al. (2014) Modulation of the organelle
376 specificity in Re(I) tetrazolato complexes leads to labeling of lipid droplets dagger. *RSC Adv*
377 4: 16345-16351.
- 378 18. Bader CA, Carter EA, Safitri A, Simpson PV, Wright P, et al. (2016) Unprecedented staining of
379 polar lipids by a luminescent rhenium complex revealed by FTIR microspectroscopy in
380 adipocytes. *Mol Biosys* 12: 2064-2068.
- 381 19. Wright PJ, Muzzioli S, Werrett MV, Raiteri P, Skelton BW, et al. (2012) Synthesis, photophysical
382 and electrochemical investigation of dinuclear tetrazolato-bridged rhenium complexes.
383 *Organometallics* 31: 7566-7578.
- 384 20. Collings DA, Carter CN, Rink JC, Scott AC, Wyatt SE, et al. (2000) Plant nuclei can contain
385 extensive grooves and invaginations. *Plant Cell* 12: 2425-2440.
- 386 21. Isaac C, Pollard JW, Meier UT (2001) Intranuclear endoplasmic reticulum induced by Nopp140
387 mimics the nucleolar channel system of human endometrium. *J Cell Sci* 114: 4253-4264.
- 388 22. Collado-Hilly M, Shirvani H, Jaillard D, Mauger JP (2010) Differential redistribution of Ca²⁺-
389 handling proteins during polarisation of MDCK cells: Effects on Ca²⁺ signalling. *Cell Calcium*
390 48: 215-224.

391 23. Rowland AA, Voeltz GK (2012) Endoplasmic reticulum-mitochondria contacts: function of the
392 junction. *Nat Rev Mol Cell Biol* 13: 607-625.

393 24. López-Sanjurjo CI, Tovey SC, Prole DL, Taylor CW (2013) Lysosomes shape Ins(1,4,5)P3-evoked
394 Ca²⁺ signals by selectively sequestering Ca²⁺ released from the endoplasmic reticulum. *J*
395 *Cell Sci* 126: 289-300.

396 25. Fagone P, Jackowski S (2009) Membrane phospholipid synthesis and endoplasmic reticulum
397 function. *J Lipid Res* 50 Suppl: S311-316.

398 26. Mor A, White MA, Fontoura BMA (2014) Nuclear trafficking in health and disease. *Curr Opin Cell*
399 *Biol* 28: 28-35.

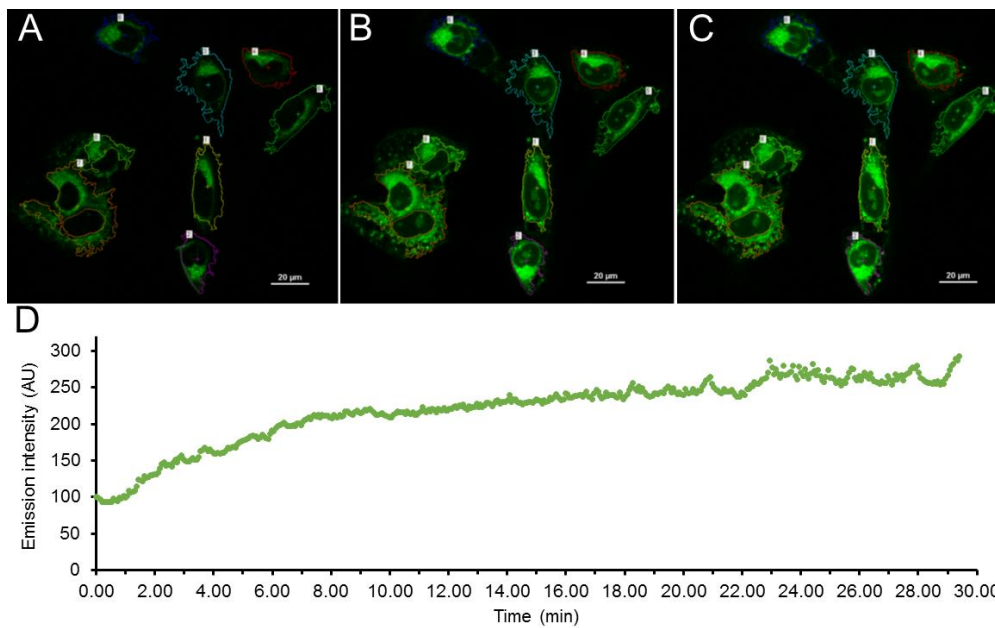
400 27. Speese SD, Ashley J, Jokhi V, Nunnari J, Barria R, et al. (2012) Nuclear envelope budding enables
401 large ribonucleoprotein particle export during synaptic Wnt signaling. *Cell* 149: 832-846.

402 28. Kilarski W, Jasinski A (1970) The formation of multivesicular bodies from the nuclear envelope. *J*
403 *Cell Biol* 45: 205-211.

404 29. Majumdar R, Tameh AT, Parent CA (2016) Exosomes mediate LTB₄ release during neutrophil
405 chemotaxis. *PloS Biol* 14: e1002336.

406

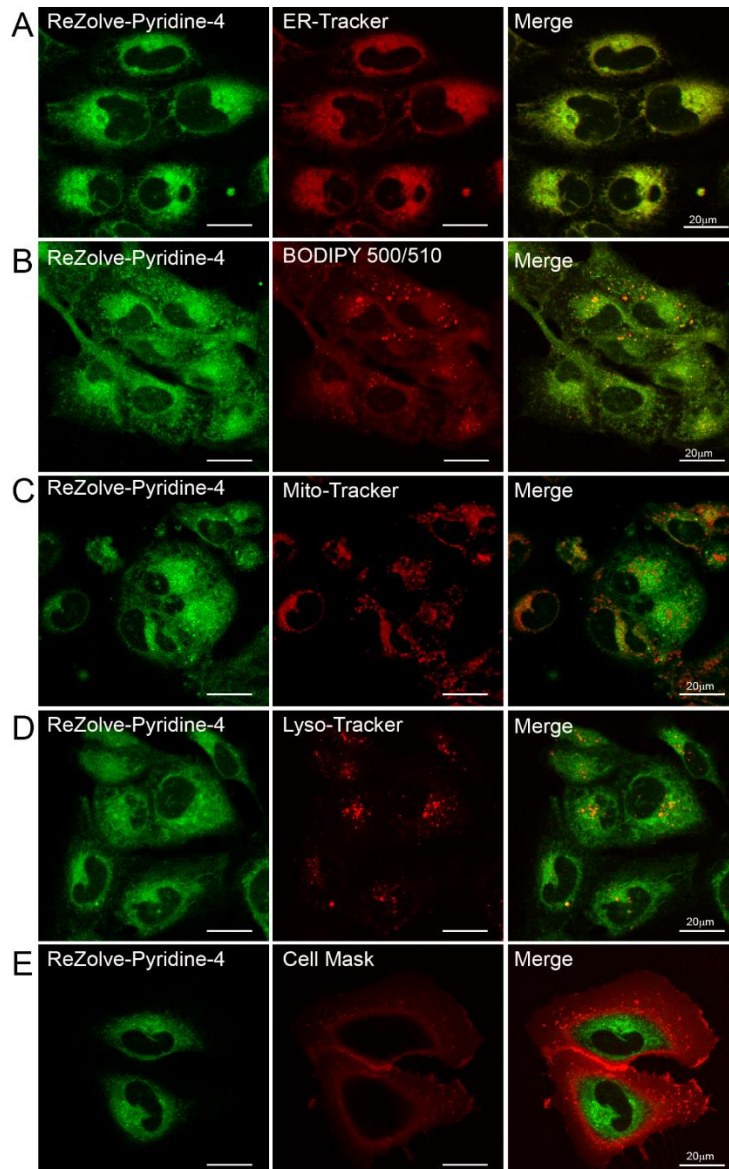
407



409

410 **Figure 1. ReZolve-ER™ does not photobleach when expose to high laser power.** (A-C)
411 *Confocal micrographs of PNT2 cells incubated with ReZolve-ER™ for 0 min (A), 15 min (B)*
412 *or 29 min (C). Overlay shows the regions of interest from which emissions intensity was*
413 *measured. (D) Scatter plot showing average emission intensity (au) of ReZolve-ER™ stained*
414 *cells from regions of interest indicated. Images collect with 403 nm excitation set to laser*
415 *power 10, a scan rate of 0.22 s (give a total of 448 scans over 29.33 min) and a pixel dwell*
416 *time of 0.22 ms.*

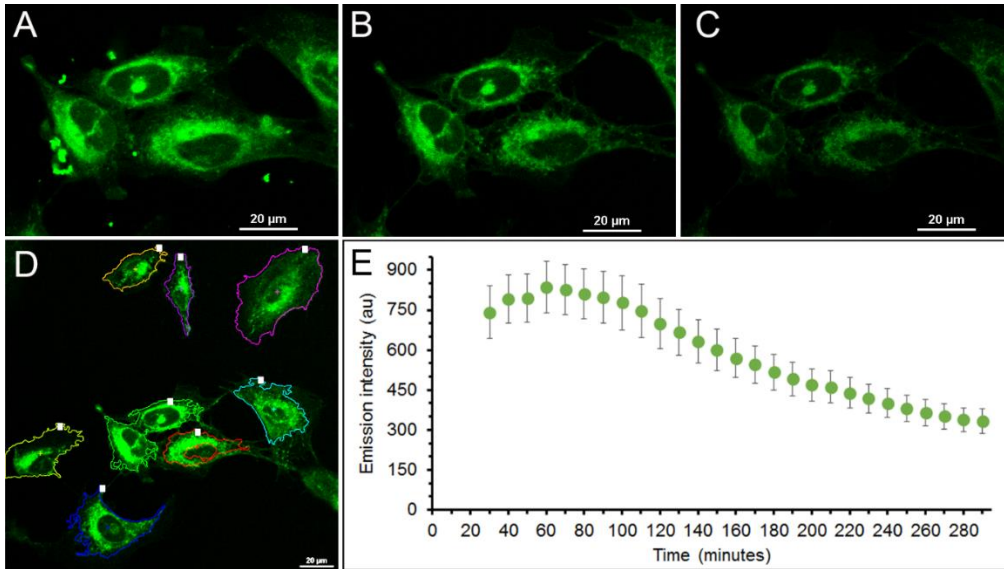
417



418

419 **Figure 2. ReZolve-ERTM subcellular localisation.** Confocal micrographs showing PNT2
 420 cells incubated with ReZolve-ERTM (green) and counter stained with (A) ER-Tracker[®] for the
 421 labelling of ER (red), (B) MitoTracker[®] for the labelling of mitochondria (red), (C)
 422 LysoTracker[®] for the labelling of lysosomes/acidic compartments (red), and (D) CellMaskTM
 423 for the labelling of the plasma membrane (red).

424

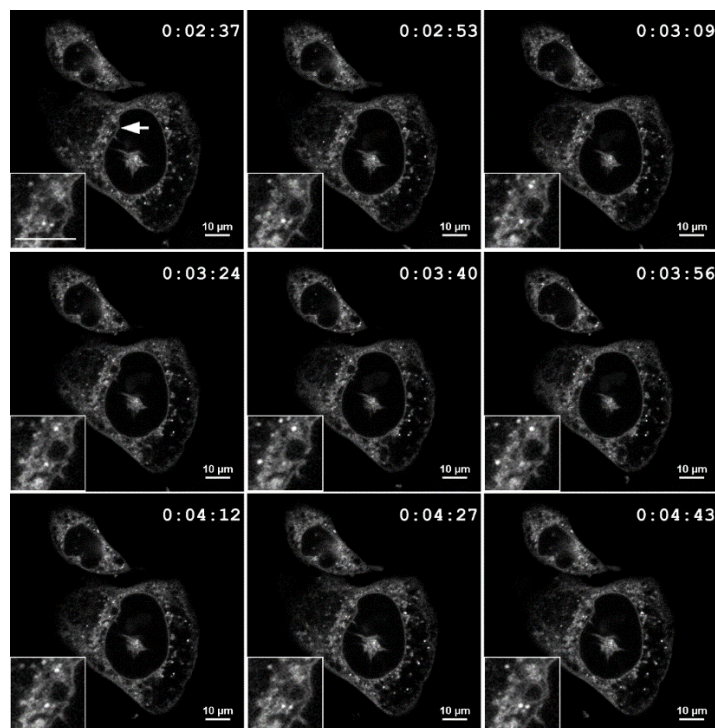


425

426 **Figure 3. ReZolve-ER™ localisation is unchanged over time.**

427 (A-D) Confocal micrographs of PNT2 cell incubated with ReZolve-ER™. Images taken at 20
 428 min (A), 140 min (B) and 290 min (C) incubation time points. (D) Shows a dot plot of
 429 emissions intensity over time. (E) Histogram of cell viability measured by an MTS assay in
 430 response to incubation with ReZolve-ER™ (Re-ER) at 50μM for 1 h, 4 h, 7 h or 24 h, when
 431 compared to a negative control of 50% DMSO in culture media (-ive control), a positive
 432 control of cells will full media (+ive control), and time point controls (control) in which cells
 433 were expose to 0.5% DMSO for 1 h, 4 h, 7 h or 24 h. * indicates a significant difference
 434 between the negative control and all other treatment conditions, ** indicates significant
 435 difference between indicated groups.

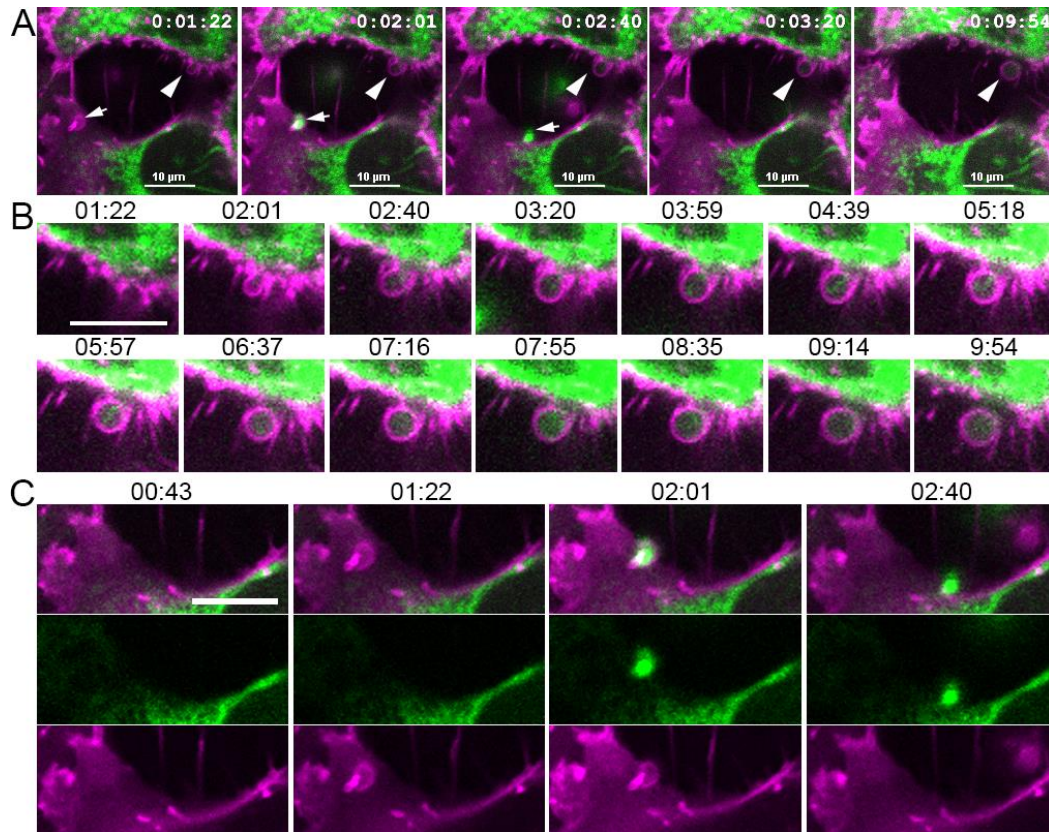
436



437

438 **Figure 4. Time lapse confocal imaging of ReZolve-ERTM in PNT2 cells.** Time of image
 439 capture is indicated in the right hand corner of each frame; and represents the last five
 440 minutes in a set of three consecutive time courses (i.e. total 15 min). Scale bar = 10 μ m.
 441 Enlarged panel shows nuclear phagosome (~ 3 μ m) forming over the time course and intense
 442 small (< 0.5 μ m) vesicular staining.

443



444

445 **Figure 5. ReZolve-ERTM imaging of vesicle release from the cell surface.** Time lapse
 446 confocal micrographs showing PNT2 cells stained with ReZolve-ERTM (green in A, B and C),
 447 counterstained with Cell Mask (purple in A, B and C). (A) Two vesicle release events were
 448 captured, arrow head indicated cross-section of budding vesicle forming which is enlarged in
 449 panel B; arrow indicates budding event at the cell surface which is enlarged in panel C. Time
 450 of capture is indicated in the right hand corner of each frame (A) or above each frame (B and
 451 C). Scale bar = 10 μ m.

452